HAL
open science

Piezoelectric Love waves on rotated Y-cut mm2 substrates

Bernard Collet, Michel Destrade

To cite this version:

Bernard Collet, Michel Destrade. Piezoelectric Love waves on rotated Y-cut mm2 substrates. IEEE Transactions on Ultrasonics, Ferroelectrics and Frequency Control, 2006, 53, pp.2132-2139. 10.1109/TUFFC.2006.153 . hal-00192237

HAL Id: hal-00192237

https://hal.science/hal-00192237v1

Submitted on 27 Nov 2007

HAL is a multi-disciplinary open access archive for the deposit and dissemination of scientific research documents, whether they are published or not. The documents may come from teaching and research institutions in France or abroad, or from public or private research centers.

L'archive ouverte pluridisciplinaire **HAL**, est destinée au dépôt et à la diffusion de documents scientifiques de niveau recherche, publiés ou non, émanant des établissements d'enseignement et de recherche français ou étrangers, des laboratoires publics ou privés.

hal-00192237, version 1 - 27 Nov 2007

Love waves in a piezoelectric layered structure

Bernard Collet and Michel Destrade

2006

Abstract

Consider a layer made of a m3m insulator crystal, with faces cut parallel to a symmetry plane. Then bond it onto a semi-infinite mm2 piezoelectric substrate. For a X- or Y-cut of the substrate, a Love wave can propagate in the resulting structure and the corresponding dispersion equation is derived analytically. It turns out that a fully explicit treatment can also be conducted in the case of a Y-cut rotated about Z. In the case of a germanium layer over a potassium niobate substrate, the wave exists at any wavelength for X- and Y-cuts but this ceases to be the case for rotated cuts, with the appearance of forbidden ranges. By playing on the cut angle, the Love wave can be made to travel faster than, or slower than, or at the same speed as, the shear bulk wave of the layer. A by-product of the analysis is the derivation of the explicit secular equation for the Bleustein-Gulyaev wave in the substrate alone, which corresponds to an asymptotic behavior of the Love wave.

1 Introduction

Layered structures, especially film/coating substrate systems, play an important role in micro-electro-mechanical systems (MEMS) and in microelectronics packages. In order to achieve high performance, many surface acoustic wave (SAW) devices/sensors are made of layered architectures such as, for instance, a dielectric, or a piezoelectric, or a non-piezoelectric semiconductor (finite-thickness) layer deposited onto a (semi-infinite) piezoelectric

substrate. For certain configurations, it is possible to have a one-component wave travel in the structure, in the direction of the interface: this guided (shear-horizontal) Love wave leaves the upper face of the layer free of mechanical tractions, its amplitude varies sinusoidally through the thickness of the layer and then decays rapidly with depth in the substrate, and it is such that all fields are continuous at the layer/substrate interface.

Love waves in piezoelectric layered acoustic devices are most suitable for high frequency filters because of their high phase velocity, and they also show great promise in bio-sensors applications with liquid environments because of their high sensitivity. Consequently, they have received much attention over the years. For example, Lardat et al. [1] found under which conditions a piezoelectrically stiffened Love wave exist and presented experimental and analytical results on surface wave delay lines. Kessenikh et al. [2] investigated surface Love waves in piezoelectric substrates of classes 6, 4, 6mm, 4mm, 622, and 422 with an isotropic dielectric layer. Hanhua and Xingjiao [3] studied Love waves for a structure made of a 6mm piezoelectric layer and a 6mm piezoelectric substrate, with a common symmetry axis in the plane of the interface, while Darinskii and Weihnacht [4] had a similar structure, made of 2mm piezoelectric layer and substrate with common symmetry axes, one of which is aligned with the propagation direction and another is aligned with the normal to the interface. Jakoby and Vellekoop [5] reviewed the properties of Love waves and associated numerical methods for a piezoelectric/piezoelectric layered structure, when the substrate is made of ST-cut quartz; so did Ogilivy [6], with special emphasis on the mass-sensitivity loading of biosensors. The reader can find additional pointers to the literature on Love waves for piezoelectric sensors in those articles and in the references therein, as well as in the reviews by Farnell and Adler [7] or by Gulyaev [8].

The present work is concerned with the propagation of Love waves in a composite structure, made of a m3m cubic insulator (non-piezoelectric semiconductor) layer of finite thickness h, bonded onto a Y-cut rotated about Z, mm2 orthorhombic, piezoelectric substrate, see Fig.1. With this singular structure, it is possible to exploit the potentiality offered by an efficient direct analytic method. The steps to be followed are: *(i)* Determine the general solution for the layer, satisfying the boundary conditions on the upper face; *(ii)* Derive some fundamental equations in the substrate using the Stroh formulation of the equations of motion there; *(iii)* Match the solutions at the layer/substrate interface; and *(iv)* Deduce the dispersion equation for piezoelectric Love waves in explicit form.

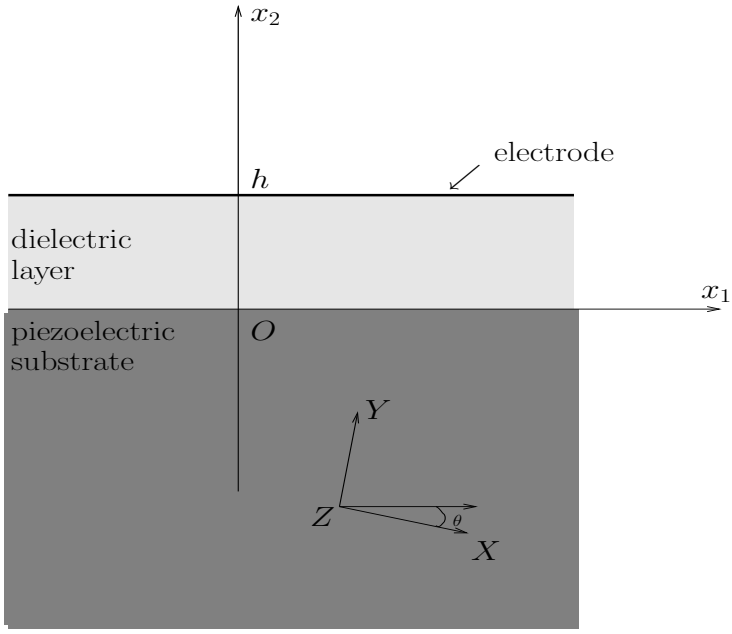

Fig. 1: Geometry of the layered structure

The dispersion relation admits a denumerable number of solutions (branches) and the solutions for the mechanical displacements, shear stresses, electric potentials, and electric inductions are deduced explicitly in the case of a metalized, mechanically free, upper surface, brought to the zero electric potential (short-circuit). In passing, the explicit secular equations for the Bleustein-Gulyaev wave speed and for the limiting wave speed (substrate only, no overlayer) are found as a cubic and as a sextic in the squared wave speed respectively, for rotated cuts. The special cases of a X-cut or Y-cut are treated separately. The effects of the angle of the cut on the phase velocity of the first modes are illustrated numerically for a specific layered structure, namely a germanium layer over a potassium niobate substrate and the appearance of a forbidden band of frequency is uncovered for a rotated cut, in sharp contrast with the non-rotated cuts where the waves exist for all frequencies.

2 The layer

First consider the upper layer, which is made of a cubic, m3m non-piezoelectric (semi-conductor) crystal, with mass density $\hat{\rho}$. For two-dimensional motions (independent of x_3), the anti-plane equation of motion decouples from its in-plane counterpart and reads ($0 \leq x_2 \leq h$)

$$\hat{c}_{44}(\hat{u}_{3,11} + \hat{u}_{3,22}) = \hat{\rho}\hat{u}_{3,tt}, \tag{1}$$

where $\hat{u}_3$ is the anti-plane mechanical displacement, $\hat{c}_{44}$ the transverse stiffness, and the comma denotes partial differentiation. For a solution in the form of an inhomogeneous wave traveling with speed v and wave number k in the x_1 direction, such as

$$\hat{u}_3 = \hat{U}_3(kx_2)\mathrm{e}^{\mathrm{i}k(x_1 - vt)}, \tag{2}$$

(where $\hat{U}_3$ is a function of kx_2 alone), the equation of motion (1) reduces to

$$\hat{U}_3'' + \left(\frac{v^2}{\hat{v}^2} - 1\right)\hat{U}_3 = 0, \qquad \text{where} \qquad \hat{v} := \sqrt{\hat{c}_{44}/\hat{\rho}}. \tag{3}$$

The general solution to this second-order differential equation is either *(i)*

$$\hat{U}_3(kx_2) = \hat{U}_3(0)\left(\cos\sqrt{\frac{v^2}{\hat{v}^2} - 1}kx_2 + A\sin\sqrt{\frac{v^2}{\hat{v}^2} - 1}kx_2\right), \quad \text{when} \quad v > \hat{v}, \tag{4}$$

or *(ii)*

$$\hat{U}_3(kx_2) = \hat{U}_3(0)\left(\cosh\sqrt{1 - \frac{v^2}{\hat{v}^2}}kx_2 + A\sinh\sqrt{1 - \frac{v^2}{\hat{v}^2}}kx_2\right), \quad \text{when} \quad v < \hat{v}, \tag{5}$$

where A is a constant to be determined from the boundary condition at $x_2 = h$. This latter condition is that the upper face of the layer be free

of mechanical tractions, so that $\hat{\sigma}_{23} = \hat{c}_{44}\hat{u}_{3,2}$ is zero there. Then it follows from (4) and (5) that: $A = \tan\sqrt{v^2/\hat{v}^2 - 1}kh$ in Case *(i)*, and that: $A = -\tanh\sqrt{1 - v^2/\hat{v}^2}kh$ in Case *(ii)*. Consequently the mechanical field is now entirely known in the layer.

The procedure to find the electrical field is similar, and even simpler because the layer is not piezoelectric. Taking the electric potential $\hat{\phi}$ in the form

$$\hat{\phi} = \hat{\varphi}(kx_2)\mathrm{e}^{\mathrm{i}k(x_1 - vt)}, \tag{6}$$

(where $\hat{\varphi}$ is a function of kx_2 alone), Poisson's equation: $\Delta\hat{\phi} = 0$ reduces to

$$\hat{\varphi}'' - \hat{\varphi} = 0, \tag{7}$$

with general solution

$$\hat{\varphi}(kx_2) = \hat{\varphi}(0)\left(\cosh kx_2 + B\sinh kx_2\right), \tag{8}$$

where B is a constant to be determined from the boundary condition on the upper face of the layer $x_2 = h$. A thin metallic film covers that face, and it is grounded to potential zero: $\hat{\varphi}(kh) = 0$. It then follows from (8) that $B = -\coth kh$, and consequently, that the electrical field is now entirely known in the layer.

For the problem at hand, only the values of the fields at the interface $x_2 = 0$ between the layer and the substrate are needed. Because the mechanical displacement $\hat{u}_3$ and the electrical potential $\hat{\phi}$ are in the forms (2) and (6), respectively, the mechanical traction $\hat{\sigma}_{23}$ and the electrical displacement $\hat{D}_2$ must also be of a similar form, due to the constitutive relations: $\hat{\sigma}_{23} = \hat{c}_{44}\hat{u}_{3,2}$ and $\hat{D}_2 = -\hat{\epsilon}_{11}\phi_{,2}$, where $\hat{\epsilon}_{11}$ is the dielectric constant of the layer. Hence,

$$\hat{\sigma}_{23} = \mathrm{i}k\hat{t}_{23}(kx_2)\mathrm{e}^{\mathrm{i}k(x_1 - vt)}, \quad \hat{D}_2 = \mathrm{i}k\hat{d}_2(kx_2)\mathrm{e}^{\mathrm{i}k(x_1 - vt)}, \tag{9}$$

(say), where $\hat{t}_{23}$ and $\hat{d}_2$ are functions of kx_2 alone. In particular, the conclusions drawn from the calculations conducted above are that at the layer/substrate interface,

$$\hat{t}_{23}(0) = -\mathrm{i}\hat{c}\hat{U}_3(0), \quad \hat{d}_2(0) = -\mathrm{i}\hat{\epsilon}\hat{\varphi}(0), \tag{10}$$

where

$$\begin{aligned}
\hat{c} &:= \hat{c}_{44}\sqrt{\frac{v^2}{\hat{v}^2}-1}\tan\sqrt{\frac{v^2}{\hat{v}^2}-1}kh, \quad \text{when} \quad v > \hat{v}, \\
\hat{c} &:= -\hat{c}_{44}\sqrt{1-\frac{v^2}{\hat{v}^2}}\tanh\sqrt{1-\frac{v^2}{\hat{v}^2}}kh, \quad \text{when} \quad v < \hat{v}, \\
\hat{\epsilon} &:= \hat{\epsilon}_{11}\coth kh.
\end{aligned} \tag{11}$$

3 The substrate

The substrate occupies the half-space $x_2 \leq 0$ and is made of the superstrong piezoelectric crystal, potassium niobate $KbNO_3$, with orthorhombic mm2 symmetry. Cut the crystal along a plane containing the Z axis and making an angle θ with the XY plane. Let $x_1x_2x_3$ be the coordinate system obtained after the rotation

$$\begin{bmatrix} m & n & 0 \\ -n & m & 0 \\ 0 & 0 & 1 \end{bmatrix}, \quad \text{where} \quad m = \cos\theta, \quad n = \sin\theta. \tag{12}$$

Yet again, for a two-dimensional motion (independent of x_3) the anti-plane strain and stress decouple from their in-plane counterparts. Hence, with $u_1 = u_2 = 0$, $u_3 = u_3(x_1, x_2, t)$ for the mechanical displacement, and $\phi = \phi(x_1, x_2, t)$ for the electric potential, the constitutive relations yield $\sigma_{11} = \sigma_{22} = \sigma_{33} = \sigma_{12} = 0$ for the stress components and $D_3 = 0$ for the electrical displacement, and they reduce to

$$\begin{aligned}
\sigma_{23} &= c_{44}u_{3,2} + c_{45}u_{3,1} + e_{14}\phi_{,1} + e_{24}\phi_{,2}, \\
\sigma_{31} &= c_{45}u_{3,2} + c_{55}u_{3,1} + e_{15}\phi_{,1} + e_{14}\phi_{,2}, \\
D_1 &= e_{14}u_{3,2} + e_{15}u_{3,1} - \epsilon_{11}\phi_{,1} - \epsilon_{12}\phi_{,2}, \\
D_2 &= e_{24}u_{3,2} + e_{14}u_{3,1} - \epsilon_{12}\phi_{,1} - \epsilon_{22}\phi_{,2},
\end{aligned} \tag{13}$$

where the c_{ij}, e_{ij}, ϵ_{ij} are related to the corresponding quantities $\tilde{c}_{ij}$, $\tilde{e}_{ij}$, $\tilde{\epsilon}_{ij}$ in the crystallographic coordinate system XYZ through tensor transformations

[9] as:

$$
\begin{aligned}
c_{44} &= m^2\tilde{c}_{44} + n^2\tilde{c}_{55}, & c_{55} &= n^2\tilde{c}_{44} + m^2\tilde{c}_{55},\\
c_{45} &= mn(\tilde{c}_{44} - \tilde{c}_{55}), & e_{24} &= m^2\tilde{e}_{24} + n^2\tilde{e}_{15},\\
e_{15} &= n^2\tilde{e}_{24} + m^2\tilde{e}_{15}, & e_{14} &= mn(\tilde{e}_{24} - \tilde{e}_{15}),\\
\epsilon_{11} &= m^2\tilde{\epsilon}_{11} + n^2\tilde{\epsilon}_{22}, & \epsilon_{22} &= n^2\tilde{\epsilon}_{11} + m^2\tilde{\epsilon}_{22},\\
\epsilon_{12} &= mn(\tilde{\epsilon}_{22} - \tilde{\epsilon}_{11}). & &
\end{aligned} \tag{14}
$$

Now consider the x_2-cut, x_1-propagation of a Shear-Horizontal interface acoustic wave that is, a motion with speed v and wave number k where the displacement field u_3 and the electric potential ϕ are of the form,

$$\{u_3, \phi\}(x_1, x_2, t) = \{U_3(kx_2), \varphi(kx_2)\}\mathrm{e}^{\mathrm{i}k(x_1 - vt)}, \tag{15}$$

(say), with

$$U_3(-\infty) = 0, \quad \varphi(-\infty) = 0. \tag{16}$$

It follows from the constitutive equations (13) that the traction σ_{32} and the electric induction D_2 are of a similar form,

$$\{\sigma_{32}, D_2\}(x_1, x_2, t) = \mathrm{i}k\{t_{32}(kx_2), d_2(kx_2)\}\mathrm{e}^{\mathrm{i}k(x_1 - vt)}, \tag{17}$$

(say), where

$$t_{32}(-\infty) = 0, \quad d_2(-\infty) = 0. \tag{18}$$

The non-trivial part of the equations of piezoacoustics, $\sigma_{ij,j} = \rho u_{i,tt}$, $D_{i,i} = 0$ (where ρ is the mass density of the crystal), can be written as a second-order differential system [10]:

$$T\begin{bmatrix} U_3'' \\ \varphi'' \end{bmatrix} + 2\mathrm{i}R\begin{bmatrix} U_3' \\ \varphi' \end{bmatrix} - [Q - (\rho v^2)J]\begin{bmatrix} U_3 \\ \varphi \end{bmatrix} = \begin{bmatrix} 0 \\ 0 \end{bmatrix}, \tag{19}$$

where the prime denotes differentiation with respect to kx_2 and

$$
\begin{aligned}
T &:= \begin{bmatrix} c_{44} & e_{24} \\ e_{24} & -\epsilon_{22} \end{bmatrix}, & R &:= \begin{bmatrix} c_{45} & e_{14} \\ e_{14} & -\epsilon_{12} \end{bmatrix},\\
Q &:= \begin{bmatrix} c_{55} & e_{15} \\ e_{15} & -\epsilon_{11} \end{bmatrix}, & J &:= \begin{bmatrix} 1 & 0 \\ 0 & 0 \end{bmatrix},
\end{aligned} \tag{20}
$$

or as a first-order differential system in the form

$$\boldsymbol{\xi}' = \mathrm{i}N\boldsymbol{\xi}, \quad \text{where} \quad \boldsymbol{\xi}(kx_2) := [U_3, \varphi, t_{31}, d_2]^t, \tag{21}$$

and N has the Stroh block structure

$$N = \begin{bmatrix} N_1 & N_2 \\ N_3 + (\rho v^2)J & N_1^t \end{bmatrix}, \tag{22}$$

with [11]

$$N_1 = -T^{-1}R, \quad N_2 = T^{-1}, \quad N_3 = RT^{-1}R - Q. \tag{23}$$

Here the components of N are easily computed from (20) and (23), by hand or using a Computer Algebra System.

Seeking a solution to (19) in the form: $[U_3, \varphi]^t = [U_3(0), \varphi(0)]^t \mathrm{e}^{\mathrm{i}kqx_2}$, where q is constant, yields the *propagation condition*

$$\det\,[q^2T + 2qR + Q - (\rho v^2)J] = 0, \tag{24}$$

a quartic in q. Explicitly,

$$c_{44}^D q^4 + 2\frac{\epsilon_{12}}{\epsilon_{22}} c_{16}^D q^3 + (c_{45}^D - \rho v^2)q^2 + 2\frac{\epsilon_{12}}{\epsilon_{22}}(c_{26}^D - \rho v^2)q + \frac{\epsilon_{11}}{\epsilon_{22}}(c_{55}^D - \rho v^2) = 0, \tag{25}$$

where

$$\begin{aligned} c_{44}^D &= c_{44} + \frac{e_{24}^2}{\epsilon_{22}}, \quad c_{16}^D = c_{44} + c_{45}\frac{\epsilon_{22}}{\epsilon_{12}} + 2\frac{e_{15}e_{24}}{\epsilon_{12}}, \\ c_{45}^D &= c_{55} + c_{44}\frac{\epsilon_{11}}{\epsilon_{22}} + 2\frac{e_{15}e_{24}}{\epsilon_{22}} + 4c_{45}\frac{\epsilon_{12}}{\epsilon_{22}} + 4\frac{e_{14}^2}{\epsilon_{22}}, \\ c_{55}^D &= c_{55} + \frac{e_{15}^2}{\epsilon_{11}}, \quad c_{26}^D = c_{55} + c_{44}\frac{\epsilon_{11}}{\epsilon_{12}} + 2\frac{e_{15}e_{24}}{\epsilon_{12}}. \end{aligned} \tag{26}$$

Out of the four possible roots, only two have a negative imaginary part, insuring exponential decay as $x_2 \to -\infty$. Computing these qualifying roots analytically is not an easy matter, because here the speed v is still an unknown. Although it is actually possible to do so [12, 13], this paper follows a different route and makes extensive use of the "fundamental equations" derived in [14–16]. They read

$$\boldsymbol{\xi}(0) \cdot M^{(n)}\overline{\boldsymbol{\xi}}(0) = 0, \quad \text{where} \quad M^{(n)} := \begin{bmatrix} 0 & I \\ I & 0 \end{bmatrix} N^n, \tag{27}$$

and n is any positive or negative integer.

4 The layer/substrate structure

The continuity of all fields at the layer/substrate interface $x_2 = 0$ imposes the boundary conditions:

$$U_3(0) = \hat{U}_3(0), \qquad \varphi(0) = \hat{\varphi}(0),$$
$$t_{23}(0) = \hat{t}_{23}(0), \qquad d_2(0) = \hat{d}_2(0). \tag{28}$$

Now the dispersion equations are derived explicitly. In the special cases of X and Y-cuts, the dispersion equation is *exact*: if it is satisfied, then the Love wave exist. In the other cases, the dispersion equation is *rationalized*: it has spurious roots, not corresponding to a true Love wave so that a subsequent validity check is necessary.

4.1 Special cases $\theta = 0, 90°$

For a X-cut or a Y-cut of the substrate, the analysis simplifies considerably and a direct treatment is possible, leading to an exact dispersion equation, and not requiring the use of the fundamental equations.

When $m = 1$, $n = 0$, or $m = 0$, $n = 1$, the parameters c_{45}, e_{14}, ϵ_{12} vanish according to (14). Then in (20), $R \equiv 0$ also, and the quartic (24) becomes the following biquadratic [4]:

$$q^4 - Sq^2 + P = 0, \tag{29}$$

where the non-dimensional quantities S and P are given by

$$-S = \frac{c_{44}\epsilon_{11} + c_{55}\epsilon_{22} + 2e_{15}e_{24} - \epsilon_{22}(\rho v^2)}{c_{44}\epsilon_{22} + e_{24}^2},$$
$$P = \frac{c_{55}\epsilon_{11} + e_{15}^2 - \epsilon_{11}(\rho v^2)}{c_{44}\epsilon_{22} + e_{24}^2}. \tag{30}$$

The relevant roots q_1 and q_2 come in one of the two following forms, either

$$(a)\ q_1 = -\mathrm{i}\beta_1,\ q_2 = -\mathrm{i}\beta_2, \qquad \text{or} \quad (b)\ q_1 = -\alpha - \mathrm{i}\beta,\ q_2 = \alpha - \mathrm{i}\beta, \tag{31}$$

where $\beta_i > 0$, $\beta > 0$. In either case, $q_1 + q_2$ has no real part and a negative imaginary part, and $q_1 q_2$ is a negative real number. Explicitly,

$$q_1 + q_2 = -\mathrm{i}\sqrt{2\sqrt{P} - S}, \quad q_1 q_2 = -\sqrt{P}. \tag{32}$$

The associated eigenvectors $\boldsymbol{\zeta^1}$ and $\boldsymbol{\zeta^2}$ follow from (for instance) the third column of the adjoints to the matrices $N - q_1 I$ and $N - q_2 I$, as $\boldsymbol{\zeta^i} = [\boldsymbol{a^i}, \boldsymbol{b^i}]^t$, $(i = 1, 2)$ where

$$\boldsymbol{a^i} = \left[q_i^2 + \frac{\epsilon_{11}}{\epsilon_{22}}, \frac{e_{24}}{\epsilon_{22}} q_i^2 + \frac{e_{15}}{\epsilon_{22}} \right]^t, \quad \boldsymbol{b^i} = q_i T \boldsymbol{a^i}, \tag{33}$$

(here T is given by (20), with components evaluated at 0° or 90°). Then the general solution to the equations of motion is of the form

$$\boldsymbol{\xi}(kx_2) = \gamma_1 \mathrm{e}^{\mathrm{i}kq_1x_2} \boldsymbol{\zeta^1} + \gamma_2 \mathrm{e}^{\mathrm{i}kq_2x_2} \boldsymbol{\zeta^2}, \tag{34}$$

where γ_1, γ_2 are disposable constants.

At $x_2 = 0$, it can be split as

$$[U_3(0), \varphi(0)]^t = A\boldsymbol{\gamma}, \quad [t_{23}(0), d_2(0)]^t = B\boldsymbol{\gamma}, \tag{35}$$

where

$$A := [\boldsymbol{a^1}|\boldsymbol{a^2}], \quad B := [\boldsymbol{b^1}|\boldsymbol{b^2}], \quad \boldsymbol{\gamma} := [\gamma_1, \gamma_2]^t. \tag{36}$$

Now the boundary conditions (28) and (10) give the link

$$\begin{aligned} B\boldsymbol{\gamma} = [\hat{t}_{23}(0), \hat{d}_2(0)]^t &= \mathrm{Diag}(-\mathrm{i}\hat{c}, -\mathrm{i}\hat{\epsilon})[\hat{U}_3(0), \hat{\varphi}(0)]^t \\ &= -\mathrm{i}\ \mathrm{Diag}(\hat{c}, \hat{\epsilon}) A\boldsymbol{\gamma}, \end{aligned} \tag{37}$$

from which the dispersion equation follows as

$$|\mathrm{i}BA^{-1} - \mathrm{Diag}(\hat{c}, \hat{\epsilon})| = 0. \tag{38}$$

It is written in this form to take advantage of the many desirable properties of the surface impedance tensor $\mathrm{i}BA^{-1}$ [24]; thus, this matrix is Hermitian in the subsonic range (defined below), and of the compact form:

$$\mathrm{i}BA^{-1} = \frac{\mathrm{i}}{q_1 + q_2} \begin{bmatrix} \rho v^2 - c_{55} - c_{44}q_1q_2 & -e_{15} + e_{24}q_1q_2 \\ -e_{15} + e_{24}q_1q_2 & \epsilon_{11} - \epsilon_{22}q_1q_2 \end{bmatrix}. \tag{39}$$

Moreover, the eigenvalues of the aggregate impedance tensor in (38) are real monotonic decreasing functions of v for any fixed kh, so that the wave speed of each mode is obtained unambiguously from the roots of (38), see Shuvalov and Every [25].

Using the identities $q_1^2 + q_2^2 = S$, $q_1^2 q_2^2 = P$ and the connections (30) and (32), the *exact, explicit, dispersion equation* is finally derived as

$$\begin{vmatrix} \dfrac{\rho v^2 - c_{55} - c_{44}\sqrt{P}}{\sqrt{2\sqrt{P} - S}} + \hat{c} & -\dfrac{e_{15} + e_{24}\sqrt{P}}{\sqrt{2\sqrt{P} - S}} \\ -\dfrac{e_{15} + e_{24}\sqrt{P}}{\sqrt{2\sqrt{P} - S}} & \dfrac{\epsilon_{11} + \epsilon_{22}\sqrt{P}}{\sqrt{2\sqrt{P} - S}} + \hat{\epsilon} \end{vmatrix} = 0, \tag{40}$$

which is a fully explicit equation, because $\hat{c}$, $\hat{\epsilon}$ are defined in (10) and S, P in (30).

The dispersion equation is valid in the *subsonic range* that is, as long as the speed is less than the *limiting speed* v_L, the smallest speed at which the biquadratic (29) ceases to have two roots q_1, q_2 with a positive imaginary part. When q_1, q_2 are of the form *(a)* in (31), then v_L is root to: $P = 0$; when they are of the form *(b)*, then v_L is root to: $2\sqrt{P} = S$. In either case, the wave becomes homogeneous at $v = v_L$ because then the roots of the biquadratic are *real*; they are: $\pm q$, where $q = \sqrt{S_L}$ or $q = \sqrt{S_L/2}$, according to each case (here S_L is S given by (30) at $v = v_L$). The associated eigenvectors are $[\boldsymbol{a}, \pm\boldsymbol{b}]^t$ where

$$\boldsymbol{a} = \left[q^2 + \frac{\epsilon_{11}}{\epsilon_{22}}, \frac{e_{24}}{\epsilon_{22}}q^2 + \frac{e_{15}}{\epsilon_{22}}\right]^t, \quad \boldsymbol{b} = qT\boldsymbol{a}. \tag{41}$$

The vanishing of the wave away from the interface can no longer be insured then, but the continuity of the fields at $x_2 = 0$ can. The conclusion is that the boundary conditions (28) and (10) lead to the following *cut-off equation*,

$$\begin{vmatrix} \left(c_{44} + \dfrac{e_{24}^2}{\epsilon_{22}}\right) q^2 + \dfrac{c_{44}\epsilon_{11} + e_{24}e_{15}}{\epsilon_{22}} & \hat{c}\left(q^2 + \dfrac{\epsilon_{11}}{\epsilon_{22}}\right) \\ e_{24}\dfrac{\epsilon_{11}}{\epsilon_{22}} - e_{15} & \hat{\epsilon}\left(\dfrac{e_{24}}{\epsilon_{22}}q^2 + \dfrac{e_{15}}{\epsilon_{22}}\right) \end{vmatrix} = 0. \tag{42}$$

This equation has an infinity of roots in kh (corresponding to the intersections of the graph of tan with the graph of coth). Each root $(kh)_L$ say, is a *cut-off parameter* for each dispersion mode, at which the Love wave ceases to exist.

Note that the dispersion equation (40) is consistent with the secular equation of a *Bleustein-Gulyaev wave* traveling in the substrate alone: as h tends to zero, $\hat{c} \to 0$, $\hat{\epsilon} \to \infty$ so that it reduces to: $\rho v^2 - c_{55} = c_{44}\sqrt{P}$, which, once

squared, coincides with the quadratic (56), obtained in the next Section. It is also consistent with the dispersion equation for a *purely elastic Love wave*. Indeed, by taking $e_{ij} \to 0$ and $\epsilon_{ij} \to 0$ in (30) and (40), the equation of Lardat et al. [1] is recovered:

$$\tan\sqrt{\frac{\hat{\rho}v^2 - \hat{c}_{44}}{\hat{c}_{44}}}kh = \frac{c_{44}\sqrt{\dfrac{c_{55} - \rho v^2}{c_{44}}}}{\hat{c}_{44}\sqrt{\dfrac{\hat{\rho}v^2 - \hat{c}_{44}}{\hat{c}_{44}}}}. \tag{43}$$

Finally, it is consistent with the dispersion equation of Love surface waves in an isotropic dielectric layer over a 6mm piezoelectric substrate [2], by the corresponding specialization.

4.2 Rotated cut

Combining the boundary conditions (28) with the results for $\hat{t}_{23}(0)$ and $\hat{d}_2(0)$ of (10) gives the following form for $\boldsymbol{\xi}(0)$:

$$\boldsymbol{\xi}(0) = U_3(0)[1, \alpha, -\mathrm{i}\hat{c}, -\mathrm{i}\hat{\epsilon}\alpha]^t, \tag{44}$$

where $\alpha := \varphi(0)/U_3(0)$ is complex: $\alpha = \alpha_1 + \mathrm{i}\alpha_2$, say. Then the fundamental equations (27) read

$$\begin{bmatrix} 1 \\ \overline{\alpha} \\ \mathrm{i}\hat{c} \\ \mathrm{i}\hat{\epsilon}\overline{\alpha} \end{bmatrix} \begin{bmatrix} M_{11}^{(n)} & M_{12}^{(n)} & M_{13}^{(n)} & M_{14}^{(n)} \\ M_{12}^{(n)} & M_{22}^{(n)} & M_{23}^{(n)} & M_{24}^{(n)} \\ M_{13}^{(n)} & M_{23}^{(n)} & M_{33}^{(n)} & M_{34}^{(n)} \\ M_{14}^{(n)} & M_{24}^{(n)} & M_{34}^{(n)} & M_{44}^{(n)} \end{bmatrix} \begin{bmatrix} 1 \\ \alpha \\ -\mathrm{i}\hat{c} \\ -\mathrm{i}\hat{\epsilon}\alpha \end{bmatrix} = 0, \tag{45}$$

or

$$\begin{aligned} &[M_{12}^{(n)} + \hat{c}\hat{\epsilon}M_{34}^{(n)}](2\alpha_1) + [\hat{\epsilon}M_{14}^{(n)} - \hat{c}M_{23}^{(n)}](2\alpha_2) \\ &\qquad + [M_{22}^{(n)} + \hat{\epsilon}^2 M_{44}^{(n)}](\alpha_1^2 + \alpha_2^2) = -[M_{11}^{(n)} + \hat{c}^2 M_{33}^{(n)}]. \end{aligned} \tag{46}$$

Writing them for $n = -1, 1, 2$, and re-arranging the three resulting equations, leads to the following non-homogeneous system of linear equations,

$$[\boldsymbol{k_1}|\boldsymbol{k_2}|\boldsymbol{k_3}]\,\boldsymbol{p} = -\boldsymbol{k_4}, \tag{47}$$

where $\boldsymbol{p} := [2\alpha_1, 2\alpha_2, \alpha_1^2 + \alpha_2^2]^t$ and $\boldsymbol{k_1}$, $\boldsymbol{k_2}$, $\boldsymbol{k_3}$, $\boldsymbol{k_4}$ are the vectors with components:

$$M_{12}^{(n)} + \hat{c}\hat{\epsilon}M_{34}^{(n)}, \quad \hat{\epsilon}M_{14}^{(n)} - \hat{c}M_{23}^{(n)}, \qquad M_{22}^{(n)} + \hat{\epsilon}^2 M_{44}^{(n)}, \quad M_{11}^{(n)} + \hat{c}^2 M_{33}^{(n)}, \tag{48}$$

$(n = -1, 1, 2)$ respectively. Cramer's rule gives the unique solution to the system as

$$2\alpha_1 = -\Delta_1/\Delta, \quad 2\alpha_2 = -\Delta_2/\Delta, \quad \alpha_1^2 + \alpha_2^2 = -\Delta_3/\Delta, \tag{49}$$

where $\Delta := \det[\boldsymbol{k_1}|\boldsymbol{k_2}|\boldsymbol{k_3}]$, $\Delta_1 := \det[\boldsymbol{k_4}|\boldsymbol{k_2}|\boldsymbol{k_3}]$, $\Delta_2 := \det[\boldsymbol{k_1}|\boldsymbol{k_4}|\boldsymbol{k_3}]$, and $\Delta_3 := \det[\boldsymbol{k_1}|\boldsymbol{k_2}|\boldsymbol{k_4}]$. The *dispersion equation* follows then from the compatibility of the equalities (49):

$$\Delta_1^2 + \Delta_2^2 + 4\Delta_3\Delta = 0. \tag{50}$$

When (and if) this dispersion relation yields a real positive wave speed v for a given wave number k, it remains to be checked whether that speed corresponds to a valid solution. Proceed as follows. First recall that the exact boundary condition is of the form (38), where now the $\boldsymbol{a^i}$, $\boldsymbol{b^i}$ $(i = 1, 2)$ are defined by

$$\begin{aligned} \boldsymbol{a^i} &:= \left[q_i^2 + 2\frac{\epsilon_{12}}{\epsilon_{22}}q_i + \frac{\epsilon_{11}}{\epsilon_{22}}, \frac{e_{24}}{\epsilon_{22}}q_i^2 + 2\frac{e_{14}}{\epsilon_{22}}q_i + \frac{e_{15}}{\epsilon_{22}}\right]^t, \\ \boldsymbol{b^i} &:= (q_i T + R)\boldsymbol{a^i}. \end{aligned} \tag{51}$$

The computation of the corresponding surface impedance tensor $\mathrm{i}BA^{-1}$ is long but perfectly possible analytically; its components depend on q_1, q_2 through the sum $q_1 + q_2$ and the product $q_1 q_2$. Now, having found a speed from (50), compute numerically the roots of the quartic (24). Select q_1 and q_2, the roots with negative imaginary parts (if there are no such roots, then v is not valid.) Then compute $q_1 + q_2$, $q_1 q_2$, and $\mathrm{i}BA^{-1}$, and check whether the exact boundary condition (38) is satisfied.

Finally, it is also possible to determine exactly the *limiting speed* v_L at which the imaginary part of an attenuation factor first vanishes. Fu [12] shows that v_L is the smallest root of $D = 0$, where D is the discriminant of the cubic resolvent associated with the quartic (24). Thus rewrite the quartic (24) in its canonical form,

$$p^4 + rp^2 + sp + t = 0, \tag{52}$$

say, using the substitution $q = p - (1/2)(\epsilon_{12}/\epsilon_{22})(c_{16}^D/c_{44}^D)$. Then,

$$D = -4(12t + r^2)^3 + (-72tr + 2r^3 + 27s^2)^2. \tag{53}$$

Here the equation $D = 0$ turns out to be a sextic in the squared wave speed, according to Maple.

5 Bleustein-Gulyaev wave as $h \to 0$

Shuvalov and Every [25] show that a great variety of asymptotic behaviors arises for an interface wave on a coated half-space, depending on whether the layer or the substrate is "fast" or "slow", or "dense" or "light", depending on which mode is under consideration, and depending on several other factors.

When the thickness of the layer vanishes here, the asymptotic behavior of the Love wave in the layer/substrate structure is that of a shear-horizontal surface wave propagation over the piezoelectric substrate alone (the Bleustein-Gulyaev wave [17, 18]). For such a wave, with metalized boundary conditions, the vector $\boldsymbol{\xi}(0)$ takes the form

$$\boldsymbol{\xi}(0) = [U_3(0), 0, 0, d_3(0)]^t = U_3(0)[1, 0, 0, \alpha]^t, \tag{54}$$

where $\alpha := d_3(0)/U_3(0)$ is complex. The fundamental equations (27), written for $n = -1, 1, 2$ (say), can be arranged as

$$\begin{bmatrix} M_{11}^{(-1)} & M_{14}^{(-1)} & M_{44}^{(-1)} \\ M_{11}^{(1)} & M_{14}^{(1)} & M_{44}^{(1)} \\ M_{11}^{(2)} & M_{14}^{(2)} & M_{44}^{(2)} \end{bmatrix} \begin{bmatrix} 1 \\ \alpha + \overline{\alpha} \\ \alpha\overline{\alpha} \end{bmatrix} = \begin{bmatrix} 0 \\ 0 \\ 0 \end{bmatrix}, \tag{55}$$

a homogeneous linear system of three equations. Its solution is non-trivial when the determinant of the 3×3 matrix on the left hand-side is zero. The resulting secular equation is a *cubic* in ρv^2. At $\theta = 0$ and $\theta = 90°$, the secular equation factorizes into the product of a term linear in ρv^2 and a term quadratic in ρv^2. In particular, at $\theta = 0$ the quadratic is:

$$(\rho v^2 - \tilde{c}_{55})^2 + \tilde{c}_{44}^2 \frac{(\rho v^2 - \tilde{c}_{55})\tilde{\epsilon}_{11} - \tilde{e}_{15}^2}{\tilde{c}_{44}\tilde{\epsilon}_{22} + \tilde{e}_{24}^2} = 0. \tag{56}$$

Now for $KbNO_3$, the material parameters of interest are [19]: $\tilde{c}_{44} = 7.43$, $\tilde{c}_{55} = 2.5$ (10^{10} N/m^2), $\tilde{e}_{24} = 11.7$, $\tilde{e}_{15} = 5.16$ (C/m^2), $\tilde{\epsilon}_{11} = 34\epsilon_0$, $\tilde{\epsilon}_{22} = 780\epsilon_0$

($\epsilon_0 = 8.854 \times 10^{-12}$ F/m), and $\rho = 4630$ kg/m^3. Using these values, the corresponding parameters in the rotated coordinate system follow from (14), and in turn, T, R, Q follow from (20), N from (22)-(23), and $M^{(n)}$ from (27). Then the cubic secular equation is solved for v for any value of the cut angle θ. Out of the three possible roots, only one may correspond to the Bleustein-Gulyaev wave (Ref. [20] explains how the adequate root is selected.) It turns out that the wave exists for all angles, with a speed v_{BG} (say) increasing from 2895.35 m/s at $\theta = 0$ to 4450.85 m/s at $\theta = 90°$. Fig.2 shows the dependence in θ, and is in agreement with the plot obtained by Nakamura and Oshiki [21] and by Mozhaev and Weihnacht [22].

Fig.2 also displays the speed of the bulk shear wave in a layer made of germanium, for which [23]: $\hat{c}_{44} = 67.1 \times 10^{10}$ N/m^2, $\hat{\epsilon}_{11} = 16.6\epsilon_0$, and $\hat{\rho} = 5330$ kg/m^3; here $\hat{v} = 3550.31$ m/s. The angle at which $v_{BG} = \hat{v}$ is $\theta_0 = 50.0817°$. Finally, the variation of the limiting speed v_L in $KbNO_3$ with the angle of cut is shown as well, and that plot is also in agreement with Mozhaev and Weihnacht [22].

6 Dispersion curves

6.1 Special case $\theta = 0°$

At $\theta = 0°$ and $kh = 0$, the interface wave travels in the substrate alone, with the Bleustein-Gulyaev wave speed of 2895.35 m/s. The limiting speed (found here as root of $2\sqrt{P} = S$) is $v_L = 3939.33$ m/s. The speed of the fundamental mode starts at the Bleustein-Gulyaev wave speed at $kh = 0$, increases to a maximum speed of about 3857.18 m/s at $kh = 0.517$, and then decreases toward the shear bulk speed of the layer, $\hat{v} = 3550.31$ m/s. In the narrow range where kh is smaller than 7.08436 $\times 10^{-2}$, the speed v of the fundamental mode wave is smaller than $\hat{v}$ and thus $\hat{c}$ is given by $(11)_2$; otherwise it is given by $(11)_1$. The fundamental mode exists for all values of kh.

The speeds of the subsequent modes start from the limiting speed v_L at $(kh)_L$ and tend to $\hat{v}$ in a monotone decreasing manner. The cut-off parameter $(kh)_L$ for the first mode, second mode , and third mode is: 6.24, 12.75, and 19.27, respectively. Fig.3 shows the dispersion curves for the fundamental mode and for the first mode. Qualitatively, the plots echo those of Kielczynski et al. [26] who considered a structure made of a 6mm substrate covered with

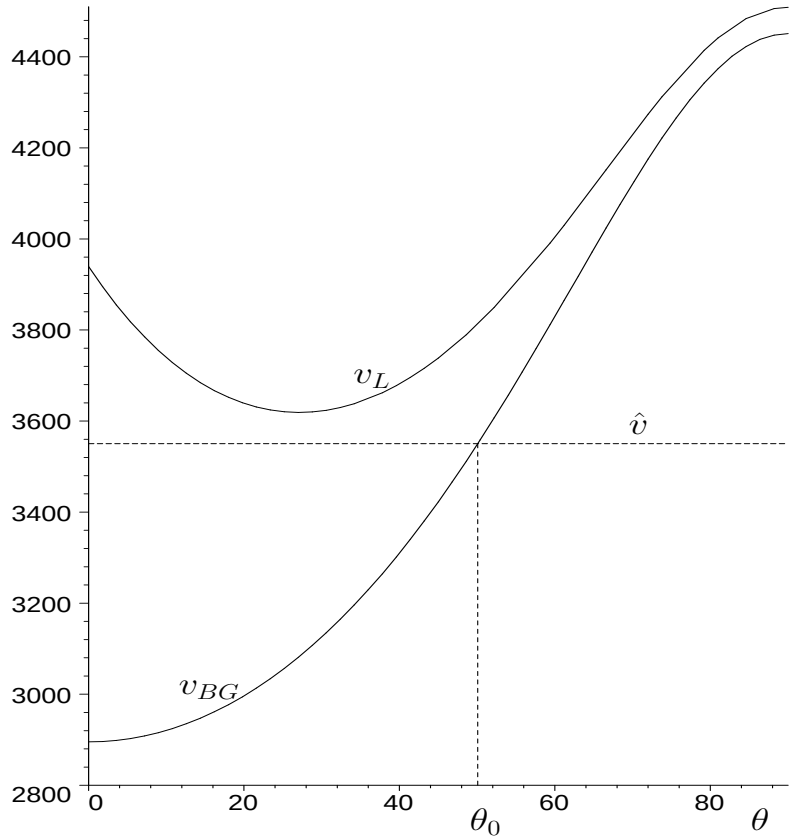

Fig. 2: Solid curves: Variations of the Bleustein-Gulyaev wave and limiting wave speeds with cut angle in a homogeneous $KbNO_3$ substrate. Dashed line: Speed of a (bulk) shear wave in germanium.

a "depolarized" layer.

6.2 Special case $\theta = 90°$

At $\theta = 90°$ and $kh = 0$ the limiting speed is root of $P = 0$; here $v_L = 4508.73$ m/s. The speed of the fundamental mode starts at the Bleustein-Gulyaev wave speed of 4450.85 m/s at $kh = 0$, increases to a maximum speed of about 4480.69 m/s at $kh = 0.0581$, and then decreases toward the shear bulk speed of the layer, $\hat{v} = 3550.31$ m/s. Here too, the fundamental mode exists for all values of kh.

The speeds of the subsequent modes start from the limiting speed v_L at $(kh)_L$ and decrease toward $\hat{v}$. The cut-off parameter $(kh)_L$ for the first mode, second mode , and third mode is: 4.05, 8.06, and 12.06, respectively. Fig.3 shows the dispersion curves for the fundamental mode and for the first and second modes.

6.3 Special case $\theta = \theta_0$

As an example of a rotated cut, consider the case where the speed of the Bleustein-Gulyaev wave in the substrate is equal to the shear wave speed in the layer; this occurs at $\theta = \theta_0 = 50.08°$, see Fig.2. For this cut the limiting speed is $v_L = 3813.36$ m/s. Starting from $v_{BG} = \hat{v}$ at $kh = 0$, the speed of the fundamental mode increases rapidly with kh. At $kh = 0.1131$, $v = v_L$ and the wave ceases to exists. This state of affairs continues until kh reaches 0.9410, after which the wave exists and its speed decreases toward $\hat{v}$. Hence a *forbidden band of frequencies* emerges for the fundamental mode, in clear contrast with the situation for non-rotated cuts. Note that the dispersion equation (50) actually gives roots below v_L in that range, which must nevertheless be discarded as they do not satisfy the exact boundary condition (38).

Here the first mode starts at the cut-off parameter $(kh)_L$ of: 8.946 with v_L and then decreases toward $\hat{v}$. Fig.4 provides a zoom into the dispersion curves of the fundamental mode around the forbidden band and of the first mode up to $kh = 12$.

In this example, the layered structure supports a shear-horizontal wave which in the long *and* short wavelength ranges travels with the speed of the layer's bulk shear wave; in the intermediate range, the wave either does not exist, or travels at a greater speed.

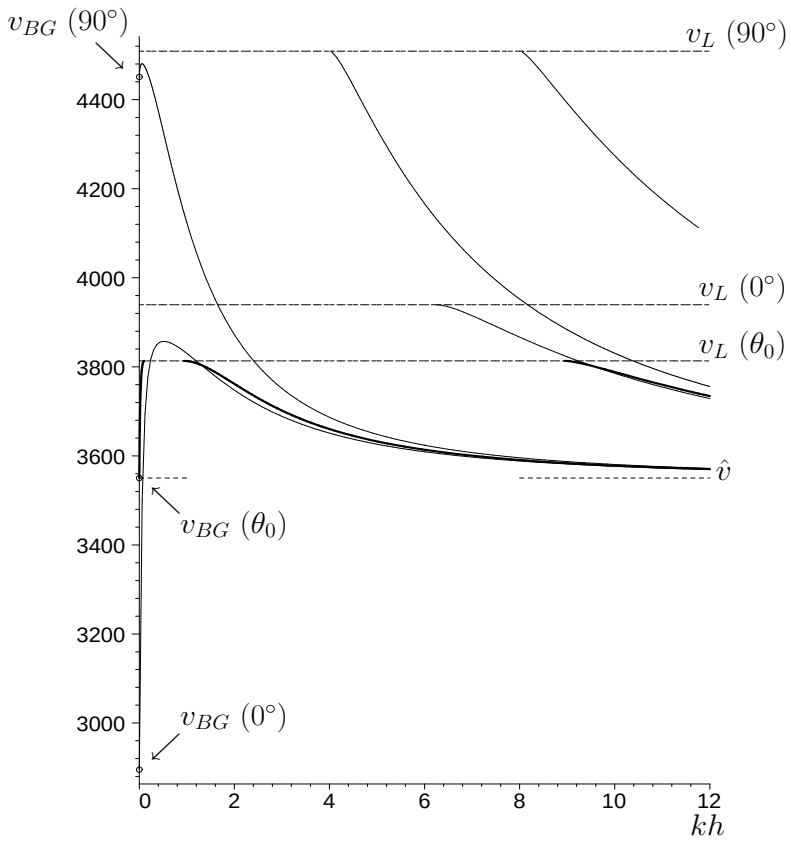

Fig. 3: Dispersion curves at $\theta = 0°, \theta_0, 90°$.

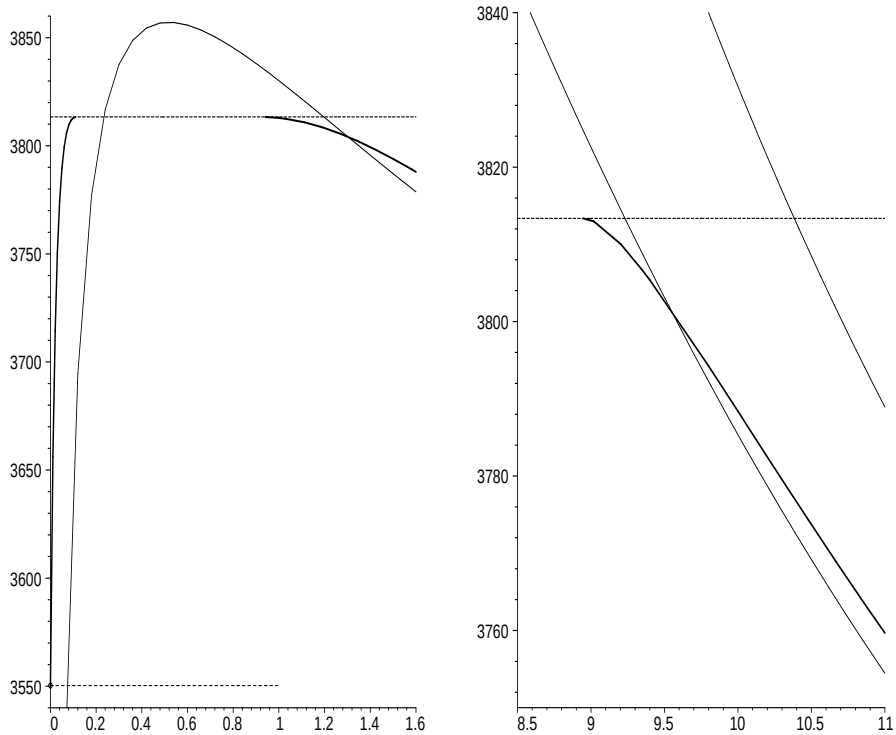

Fig. 4: Zooms for the dispersion of (a) the fundamental mode and (b) the first mode at $\theta = \theta_0$ (thin curves) and at $\theta = 0°, 90°$ (thick curves) .

References

[1] C. Lardat, C. Maerfeld, and P. Tournois, "Theory and performance of acoustical dispersive surface wave delay lines," *Proc. IEEE*, vol.59, pp. 355–368, 1971.

[2] G. G. Kessenikh, V. N. Lyubimov, and L. A. Shuvalov, "Love surface waves in piezoelectrics," *Sov. Phys. Crystallogr.*, vol. 27, pp. 267–270, 1982.

[3] F. Hanhua and L. Xingjiao, "Shear-horizontal surface waves in a layered structure of piezoelectric ceramics," *IEEE Trans. Ultrason. Ferro. Freq. Control*, vol. 40, pp. 167–170, 1993.

[4] A. N. Darinskii and M. Weihnacht, "Supersonic Love waves in strong piezoelectrics of symmetry $mm2$," *J. Appl. Phys.*, vol. 90, pp. 383–388, 2001.

[5] B. Jakoby and M. J. Vellekoop, "Properties of Love waves: applications in sensors," *Smart Mater. Struct.*, vol. 6, pp. 668–679, 1997.

[6] J. A. Ogilvy, "The mass-loading sensitivity of acoustic Love waves biosensors in air," *J. Phys. D: Appl. Phys.*, vol. 30, pp. 2497–2501, 1997.

[7] G. W. Farnell and E. L. Adler, "Elastic wave propagation in thin layers," in *Physical Acoustics*, vol. 9, W. P. Mason and R. N. Thurston, Eds. New York: Academic Press, 1972, pp. 35–127.

[8] Yu. V. Gulyaev, "Review of shear surface acoustic waves in solids," *IEEE Trans. Ultrason. Ferro. Freq. Control*, vol. 45, pp. 935–938, 1998.

[9] B. A. Auld, *Acoustic fields and waves in solids.* Malabar, FL: Krieger, 1990, p. 275.

[10] V. G. Mozhaev and M. Weihnacht, "Sectors of nonexistence of surface acoustic waves in potassium niobate," in *Proc. IEEE Ultrasonics Symp.* 2002, vol. 1, pp. 391–395.

[11] T. C. T. Ting, *Anisotropic elasticity: theory and applications.* New York: Oxford University Press, 1996.

[12] Y. B. Fu, "An explicit expression for the surface-impedance matrix of a generally anisotropic incompressible elastic material in a state of plane strain," *Int. J. Non-linear Mech.*, vol. 40, pp. 229–239, 2005.

[13] M. Destrade and Y. B. Fu, "The speed of interface waves polarized in a symmetry plane," *Int. J. Eng. Sc.*, vol. 44, pp. 26–36. 2006.

[14] M. Destrade, "Elastic interface acoustic waves in twinned crystals," *Int. J. Solids Struct.*, vol. 40, pp. 7375–7383, 2003.

[15] M. Destrade, "Explicit secular equation for Scholte waves over a monoclinic crystal," *J. Sound Vibr.*, vol. 273, pp. 409–414, 2004.

[16] M. Destrade, "On interface waves in misoriented pre-stressed incompressible elastic solids," *IMA J. Appl. Math.*, vol. 70, pp. 3–14, 2005.

[17] J. L. Bleustein, "A new surface wave in piezoelectric materials," *Appl. Phys. Lett.*, vol. 13, pp. 412–413, 1968.

[18] Yu. V. Gulyaev, "Electroacoustic surface waves in piezoelectric materials", *JETP Lett.*, vol. 9, pp. 37–38, 1969.

[19] M. Zgonik, R. Schlesser, I. Biaggio, E. Voit, J. Tscherry, and P. Günter, "Material constants of $KNbO_3$ relevant for electro- and acousto-optics," *J. Appl. Phys.*, vol. 74, p. 1287, 1993.

[20] B. Collet and M. Destrade, "Explicit secular equations for piezoacoustic surface waves: Shear-Horizontal modes," *J. Acoust. Soc. Am.*, vol. 116, pp. 3432–3442, 2004.

[21] K. Nakamura and M. Oshiki, "Theoretical analysis of horizontal shear mode piezoelectric surface acoustic waves in potassium niobate," *Appl. Phys. Lett.*, vol. 71, pp. 3203–3205, 1997.

[22] V. G. Mozhaev and M. Weihnacht, "Incredible negative values of effective electromechanical coupling coefficient for surface acoustic waves in piezoelectrics," *Ultrasonics*, vol. 37, pp. 687–691, 2000.

[23] W. Martienssen and H. Warlimont, Eds. *Springer Handbook of Condensed Matter and Materials Data.* Berlin: Springer, 2005.

[24] M. Abbudi and D. M. Barnett, "On the existence of interfacial (Stoneley) waves in bonded piezoelectric half-spaces," *Proc. Roy. Soc. London A*, vol. 429, pp. 587–611, 1990.

[25] A. L. Shuvalov and A. G. Every, "Some properties of surface acoustic waves in anisotropic-coated solids, studied by the impedance method," *Wave Motion*, vol. 36, pp. 257–273, 2002.

[26] P. J. Kielczynski, W. Pajewski, and M. Szalewski, "Shear-horizontal surface waves on piezoelectric ceramics with depolarized surface layer," *IEEE Trans. Ultras. Ferroelec. Freq. Control*, vol. 36, pp. 287- 293, 1989.